

Blue-Noise Sampling on Graphs

Alejandro Parada-Mayorga, Daniel L. Lau, *Senior Member, IEEE*, Jhony H. Giraldo, and Gonzalo R. Arce, *Fellow, IEEE*,

Abstract—In the area of graph signal processing, a graph is a set of nodes arbitrarily connected by weighted links; a graph signal is a set of scalar values associated with each node; and sampling is the problem of selecting an optimal subset of nodes from which any graph signal can be reconstructed. For small graphs, finding the optimal sampling subset can be determined by looking at the graph’s Fourier transform; however in some cases the spectral decomposition used to calculate the Fourier transform is not available. As such, this paper proposes the use of a spatial dithering, on the graph, as a way to conveniently find a statistically good, if not ideal, sampling – establishing that the best sampling patterns are the ones that are dominated by high frequency spectral components, creating a power spectrum referred to as blue-noise. The theoretical connection between blue-noise sampling on graphs and previous results in graph signal processing is also established, explaining the advantages of the proposed approach. Restricting our analysis to undirected and connected graphs, numerical tests are performed in order to compare the effectiveness of blue-noise sampling against other approaches.

Index Terms—Blue-noise sampling, graph signal processing, signal processing on graphs, sampling sets.

I. INTRODUCTION

Interesting phenomena in nature can often be captured by graphs since objects and data are invariably inter-related in some sense. Social [1], financial [2], ecological networks, and the human brain [3] are a few examples of such networks. Data in these networks reside on irregular or otherwise unordered structures [4]. New data science tools are thus emerging to process signals on graph structures where concepts of algebraic and spectral graph theory are being merged with methods used in computational harmonic analysis [5], [6], [7]. A feature that these networks of interest have in common, is that they define very large graphs [8]. Their scale is in the tens of thousands, if not millions, of nodes and edges that describe their relationships [9].

Algorithms to compute the shortest path, centrality, spectra, clustering and many other descriptors of a complete graph, rapidly become impractical when the graphs under study become large [9], [10]. Graph sampling thus becomes essential. Naturally, the mathematics of sampling theory and spectral

graph theory have been combined leading to generalized Nyquist sampling principles for graphs [5], [11], [12], [13]. In general, these methods are based on the assumption that the underlying graph spectral decompositions are known and available in advance [14], [15]. In many applications of interest, however, the graphs structures are massive, dynamic, and their spectral decompositions are computationally overwhelming if not unfeasible.

This work explores a somewhat radical departure from prior work by relying on the assumption that the graph spectrum is not known or its calculation is computationally expensive. Specifically, we intend to design graph signal sampling techniques that promote the minimization of low frequency energy of the sampling patterns on the original graph to produce what is referred to in the spatial dithering literature as *blue-noise* [16], [17]. Furthermore; low computational complexity dither algorithms are developed that closely mimic the ideal patterns by using techniques modeled after error-diffusion, a derivation of sigma-delta modulation for generating halftone images [18], [17]. With sufficient sampling rates, error-diffusion has been used to generate optimal stochastic sampling grids for preserving circular bandlimited signals [19], [20], [21], [22]. Although not well understood nor readily practiced in place of fixed-time/space sampling in traditional signal and image processing applications [23], [24], the notion of stochastic sampling is compelling for graphs since graphs do not have a concept of equal spacing in time or space.

In this paper, the connection between the properties of blue-noise sampling patterns and the results related with sampling sets in graphs is established, showing that blue-noise like sampling patterns in graphs are connected with good sampling sets in terms of preserving the uniqueness of the representation of the sampled signal. A new numerical algorithm is proposed in order to compute these blue-noise patterns based on the spectral characteristics and the spatial distribution of the patterns. In particular, trying to exploit the distribution of the sampling points on the nodes of the graph, a void and cluster algorithm on graphs is developed [25], allowing the generation of patterns that lead to reconstruction errors of bandlimited signals, similar or in some cases superior to the ones obtained in the state-of-the-art literature.

This work is organized as follows. In Section II, notation and basic concepts about signal processing on graphs are stated presenting also a description of previous approaches about sampling on graphs. In Section III blue-noise sampling on graphs is discussed. In Section IV an algorithm for the generation of blue-noise patterns is discussed, whereas in Section V a set of numerical tests show the performance of the proposed algorithm against other techniques. Finally, in Section VI a set of conclusions is presented.

Alejandro Parada-Mayorga and Jhony H. Giraldo are with the Department of Electrical and Computer Engineering, University of Delaware, Newark, DE, 19716 USA e-mail: alejopm@udel.edu.

Daniel L. Lau is with the Department of Electrical and Computer Engineering, University of Kentucky, Lexington, Kentucky, 40526 USA e-mail: dllau@uky.edu.

Gonzalo R. Arce is with Institute for Financial Services Analytics and the Department of Electrical and Computer Engineering, University of Delaware, Newark, DE, 19716 USA e-mail: alejopm@udel.edu, arce@udel.edu.

This work was supported in part by the National Science Foundation, grant NSF #1815992, by the UDRF foundation strategic initiative award, and by a University of Delaware Dissertation Fellowship Award.

II. PRELIMINARIES

Sandryhaila et. al [26], proposed a theoretical framework for the analysis and processing of signals on graphs based on the properties of the adjacency matrix. This approach is rooted in *algebraic signal processing*, whereas authors like Fuhr and Pesenson [27], [11], [12], Puy [28] and Shuman [5], [6], [29] based their analysis of signals on graphs, relying on the properties of the *Laplacian matrix*. In both approaches the Fourier transform of the signals on the graph is defined in terms of a spectral decomposition of the adjacency matrix and the Laplacian matrix respectively, using the set of eigenvectors as the Fourier basis for the representation of the signals.

The first approach offers a direct connection with the shift operator used in traditional signal processing, while the second resembles the main ideas of Fourier analysis in linear spaces in which the eigenfunctions of the Laplacian operator are used as the basis representation of the signal. The two approaches use a unitary operator, and problems like sampling and filtering can be successfully considered in both scenarios. In this work, the combinatorial Laplacian matrix is used as the building block. Consequently part of the developments proposed rely on the theoretical results obtained by Furh and Pesenson [27], [11], [12] in harmonic analysis on graphs.

A. Graph Sampling

Let $G = (\mathcal{V}, \mathcal{E})$ be an undirected weighted graph with a set of nodes, \mathcal{V} , and a set of edges, \mathcal{E} . \mathbf{W} is the adjacency matrix (symmetric), with $\mathbf{W}(u, v)$ the weight connecting the nodes u and v . The degree matrix, \mathbf{D} , is a diagonal matrix whose entries are given according to:

$$\mathbf{D}(u, u) = \sum_{v \neq u} \mathbf{W}(v, u). \quad (1)$$

On the graph G , the combinatorial Laplacian operator is defined as the positive semi-definite operator:

$$\mathbf{L} = \mathbf{D} - \mathbf{W}, \quad (2)$$

whose eigenvalues are organized as $0 \leq \mu_1 \leq \mu_2 \leq \dots \leq \mu_N$, $N = |\mathcal{V}|$ [30]. In particular for each component of the Laplacian, it follows that:

$$(\mathbf{L}\mathbf{x})(v) = \sum_{u \in \mathcal{V}} (\mathbf{x}(v) - \mathbf{x}(u)) \mathbf{W}(v, u), \quad (3)$$

where, if G is connected, $\mu_1 = 0$ and $\mu_\ell > 0$ for all $\ell > 1$ [30]. A real signal, \mathbf{x} , on the graph is then defined as the mapping $\mathbf{x} : \mathcal{V} \rightarrow \mathbb{R}$ represented by the vector $\mathbf{x} \in \mathbb{R}^N$ where $\mathbf{x}(v)$ is the value of the signal associated to $v \in \mathcal{V}$. The support of \mathbf{x} is represented as $\text{supp}(\mathbf{x})$.

If the spectral decomposition of the operator, \mathbf{L} , is represented as $\mathbf{L} = \mathbf{U}\mathbf{\Lambda}\mathbf{U}^T$, then the Graph Fourier Transform of the signal, \mathbf{x} on G , is given by $F\{\mathbf{x}\} = \hat{\mathbf{x}} = \mathbf{U}^T\mathbf{x}$. There is a direct analogy between the concept of frequency in traditional Fourier Analysis and the behavior of the Graph Fourier Transform as is stated in [5]. Considering this analogy, the bandwidth of a signal \mathbf{x} can be defined using the nonzero components of $\hat{\mathbf{x}}$. It is said that \mathbf{x} has bandwidth $\omega \in \mathbb{R}_+$ if $\hat{\mathbf{x}} \in PW_\omega(G) = \text{span}\{\mathbf{U}_k : \mu_k \leq \omega\}$, where $PW_\omega(G)$ is the

Paley-Wiener space of bandwidth ω [11] and \mathbf{U}_k indicates the first k column vectors in \mathbf{U} .

Given a notion of bandwidth, one invariably questions the notion of sampling rate and can the number of samples or nodes of a graph be reduced without loss of information to the signal? We, therefore, define sampling of a signal \mathbf{x} on the graph G , by choosing the components of \mathbf{x} on a subset of nodes, $\mathcal{S} = \{s_1, \dots, s_m\} \subset \mathcal{V}$. The sampled signal is given by $\mathbf{x}_\mathcal{S} = \mathbf{M}\mathbf{x}$ where \mathbf{M} is a binary matrix whose entries are given by $\mathbf{M} = [\delta_{s_1}, \dots, \delta_{s_m}]^T$ and δ_v the N -dimensional Kronecker column vector centered at v . Given $\mathbf{x}_\mathcal{S}$, it is possible to obtain a reconstructed version of \mathbf{x} in different ways depending on whether the bandwidth of the signal is known. We assume that the bandwidth is known with the reconstruction given by:

$$\mathbf{x}_{rec} = \underset{\mathbf{z} \in \text{span}(\mathbf{U}_k)}{\text{argmin}} \|\mathbf{M}\mathbf{z} - \mathbf{x}_\mathcal{S}\|_2^2 = \mathbf{U}_k (\mathbf{M}\mathbf{U}_k)^\dagger \mathbf{x}_\mathcal{S} \quad (4)$$

where $(\mathbf{M}\mathbf{U}_k)^\dagger$ is the Moore-Penrose pseudo-inverse of $\mathbf{M}\mathbf{U}_k$ [31], [32].

The problem of optimally sampling a signal on a graph can now be summarized as choosing \mathcal{S} such that we maximize the available bandwidth of $\mathbf{x}_\mathcal{S}$. To this end, Pesenson defines [11], [12] a Λ -removable set for $\Lambda > 0$ as the subset of nodes, $\mathcal{S} \subset \mathcal{V}$, for which:

$$\|\mathbf{x}\|_2 \leq (1/\Lambda)\|\mathbf{L}\mathbf{x}\|_2 \quad \forall \mathbf{x} \in L_2(\mathcal{S}). \quad (5)$$

where $L_p(\mathcal{S})$, $p = 1, 2, \dots$ is the set of all signals, \mathbf{x} , with support in $\mathcal{S} \subset \mathcal{V}$ (i.e. elements of \mathbf{x} not included in \mathcal{S} are equal to zero) and finite l_p norm. The best value of the constant, obtained from $\inf_\Lambda(1/\Lambda)$, is denoted by $\Lambda_\mathcal{S}$. Notice that for any subset of nodes, there exists a Λ -removable set with larger or smaller $\Lambda_\mathcal{S}$. So $\Lambda_\mathcal{S}$ ultimately determines how much importance a given set has in the sampling process of a signal with a specific bandwidth.

The relationship between properties of removable sets and the sampling problem was established by Pesenson in the following theorem:

Theorem 1 (Theorem 5.1 in [11])

If for a set $\mathcal{U} \subset \mathcal{V}$, its compliment $\mathcal{U}^c = \mathcal{V} \setminus \mathcal{U}$ is a $\Lambda_{\mathcal{U}^c}$ -removable set, then all signals in $PW_\omega(G)$ are completely determined by its values in \mathcal{U} , whenever $0 < \omega < \Lambda_{\mathcal{U}^c}$.

In [27], another result related with sampling sets is established using a constant that can be calculated directly with the weights, \mathbf{W} , of the graph, G , stated in the following theorem:

Theorem 2 ([27])

Every $\mathcal{S} \subset \mathcal{V}$ is a sampling set for all functions in $PW_\omega(G)$ with any $\omega < K_\mathcal{S}$, where

$$K_\mathcal{S} = \inf_{v \in \mathcal{S}^c} w_\mathcal{S}(v) \quad (6)$$

and $w_\mathcal{S}(v) = \sum_{s \in \mathcal{S}} \mathbf{W}(s, v)$.

Theorems 1 and 2 play a central role in the description of properties for different classes of sampling sets as it is possible to consider that a *good* sampling set, \mathcal{S} , promotes the

maximization of constants, Λ_{S^c} and K_S . In particular, it will be shown in the following sections that blue-noise sampling patterns indeed promote higher values of these constants with respect to random sampling.

B. Optimal Graph Sampling

The problem of finding the best \mathcal{S} is a combinatorial problem of calculating Λ_{S^c} for all sampling sets and choosing the set with the largest value of Λ_{S^c} , a prohibitively expensive process for larger graphs. Allowing for some short cuts, a simple, greedy, procedure for finding a good sampling set starts with an empty set of nodes and iteratively adds one node at a time, taking the best available node at each iteration according to the value of a cost function. Several authors have formulated the problem of sampling and reconstruction in the presence of measurement noise, and in these works, objective functions have been proposed that minimize the reconstruction error in terms of the worst case [15], where $\mathcal{S}^{opt} = \arg \max_{|\mathcal{S}|=m} \sigma_1^2$, the mean case [31], where $\mathcal{S}^{opt} = \arg \max_{|\mathcal{S}|=m} \sum_{i=1}^{\min\{m,k\}} \sigma_i^{-2}$, and the maximum volume case [32], where $\mathcal{S}^{opt} = \arg \max_{|\mathcal{S}|=m} \prod_{i=1}^{\min\{m,k\}} \sigma_i^2$, and σ_i represents the i^{th} singular value of the matrix $\mathbf{M}\mathbf{U}_k$ consisting of the first k eigenvectors of \mathbf{W} or \mathbf{L} respectively, sampled on the rows indicated by \mathcal{S} .

In order to reduce computational complexity, Anis et. al. [31] defines *graph spectral proxies* of order q as estimates of the cutoff frequency of a given signal which can be used to define cutoff frequency estimates for a subset of nodes \mathcal{S} according to:

$$\Omega_q(\mathcal{S}) = \min_{\phi \in L_2(\mathcal{S}^c)} \left(\frac{\|\mathbf{L}^k \phi\|_2}{\|\phi\|_2} \right)^{\frac{1}{q}}, \quad (7)$$

with \mathbf{L}^q being the q^{th} power of \mathbf{L} [31], [14]. Anis et. al. further shows that, for any $q \in \mathbb{N}$ and \mathcal{S} , it is possible to have perfect reconstruction when $\omega < \Omega_q(\mathcal{S})$. The value of $\Omega_q(\mathcal{S})$ can be calculated as $\Omega_q(\mathcal{S}) = (\sigma_{1,q})^{\frac{1}{2q}}$, where $\sigma_{1,q}$ denotes the smallest eigenvalue of the reduced matrix $(\mathbf{L}_{\mathcal{S}^c, \mathcal{S}^c}^T)^q \mathbf{L}_{\mathcal{S}^c, \mathcal{S}^c}^q$. The optimal sampling set can then be represented as the solution of the problem:

$$\mathcal{S}_q^{opt} = \arg \max_{|\mathcal{S}|=m} \Omega_q(\mathcal{S}), \quad (8)$$

which is still combinatorial; however, Anis et. al. proposes a heuristic rule to solve eqn. (8) using the first eigenvector of the spectral decomposition of the matrix, $\mathbf{L}_{\mathcal{S}^c, \mathcal{S}^c}^q$. Basically, a node is added to the sampling set according to the index of the component with the maximum absolute value of the first eigenvector of $\mathbf{L}_{\mathcal{S}^c, \mathcal{S}^c}^q$. The quality of the sampling set is also related to the value of q which should be selected as large as possible at the expense of a higher computational cost.

In some scenarios for sampling signals on graphs a spectral decomposition of the operators is not available, and therefore there is a strong need for vertex domain sampling schemes that attempt to build good sampling patterns based entirely on the local graph structure around a node. So for these cases where the graphs are too large for calculating the eigenvalues and eigenvectors of the GFT, several authors have looked at the

problem of sampling graphs that may not be optimal but are still very good at preserving band-limited signals. In the case of Puy et. al [28], a random sampling technique is proposed, where the authors propose a random selection of nodes with a recovery algorithm that involves a probability distribution diagonal matrix, \mathbf{P} , in addition to the sampling matrix operator \mathbf{M} . The reconstructed signal \mathbf{x}_{rec} can then be calculated as:

$$\mathbf{x}_{rec} = \arg \min_{\mathbf{z} \in \mathbb{R}^N} \left(\left\| \mathbf{P}^{-1/2} (\mathbf{M}\mathbf{z} - \mathbf{x}_S) \right\|_2^2 + \tau \mathbf{z}^T \mathbf{L}^r \mathbf{z} \right), \quad (9)$$

where $\mathbf{x}_S = \mathbf{M}\mathbf{x}$ is the sampled version of the signal \mathbf{x} and τ is a regularization parameter selected empirically.

Puy et. al [28] further show that an optimal \mathbf{P} can be determined by the use of the *local graph coherence*, ν_k , on the nodes of the graph. The value of $\nu_k(i)$ at the node i can be calculated as $\nu_k(i) = \|\mathbf{U}_k \boldsymbol{\delta}_i\|_2$, where $\boldsymbol{\delta}_i$ is the Kronecker vector centered at node i , and it provides a measure about how important is the node i for the sampling of a signal with bandwidth k . If $\nu_k(i)$ in these first k coefficients is equal to 1 for a particular node, then there exists k -bandlimited graph signals whose energy is solely concentrated in this i^{th} node. If the energy is 0, then no k -band-limited graph signal has any energy in this i^{th} node. So node i can be deleted with no repercussions.

Because the calculation of $\nu_k(i)$ requires the knowledge of the spectral decomposition, Puy et. al propose an approximate estimation of $\nu_k(i)$ that can be obtained without the calculation of any spectral decomposition, which allows the solution of eqn. (9). When the optimal \mathbf{P} is used, Puy et. al show that the matrix $\mathbf{M}\mathbf{P}^{-1/2}$ satisfies a restricted isometry property when the number of samples is on the order of $O(k \log k)$, which provides a strong guarantee for the exact recovery of the signal. This represents an elegant result but with the drawback that $O(k \log k)$ is substantially higher than k , which is the optimal number of samples required to reconstruct a signal of bandwidth k .

Recently, Tremblay et. al. [32] proposes the use of *determinantal point processes (DPP)* in order to obtain the matrix \mathbf{P} used in [28]. It is shown in [32] that an optimal \mathbf{P} can be obtained using DPP when \mathbf{U}_k is known. Additionally, when the spectral decomposition is not accessible it is shown how a variant of the Wilson's Algorithm introduced in [33] can be used in order to obtain a sampling set that can be shown it is related with a DPP that leads to an approximate version of the optimal \mathbf{P} . The reconstruction of the signal is obtained by the solution of eqn. (9). However these results do not represent an improvement with respect to Anis et. al. [31] or Chen et. al. [15] and may lead to larger reconstruction errors when the graph considered does not have a strong community graph structure [32].

Marques et. al [34], proposed a different approach with respect to previous works, considering the sampling and reconstruction of the signal using its samples on a single node. The central idea is based on the information provided by the sequential application of the shift operator. The technique itself represents a remarkable new alternative with potential applications in network analysis and its computational cost may be a drawback when large size graphs are considered.

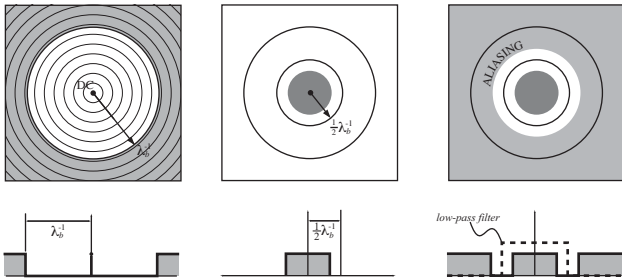


Fig. 1: Sampling and reconstruction showing (left) the power spectrum of the blue-noise sampling grid, (center) the circular band-limited surface to be sampled, and (right) spectral representation of the sampled signal with the ideal reconstruction filter illustrated by the dashed line.

III. BLUE-NOISE SAMPLING ON GRAPHS

This work proposes a different approach to graph signal sampling: the application of spatial dithering to the graph vertex domain where, the spectral properties of well formed sampling patterns will equally benefit the graph vertex domain as they do the spatial. This approach is motivated by the well established research in digital halftoning [18], [17], which is the process of converting a continuous tone image or photograph into a pattern of printed and not-printed dots for reproduction by inkjet or laser printers [16]. Halftoning algorithms based on error-diffusion are of particular importance because they produce random patterns of homogeneously distributed dots where minority pixels (black dots in highlights or white dots in shadows) are spaced as far apart as possible. These patterns have power spectra dominated by high frequency energy, earning the name, “blue-noise,” since blue is the high frequency component of white light. Low frequency energy or red-noise contributes to halftone patterns looking fuzzy or noisy to the human visual system and are, therefore, to be avoided [16], [18].

For graph signal sampling, blue-noise dithering offers several immediately valuable attributes. First in terms of traditional image sampling and reconstruction, ideal blue-noise patterns form an upside-down round hat spectrum with a dirac delta at the origin of the Fourier plane [19]. So sampling of a circular band-limited signal results in a signal that can be perfectly reconstructed by means of an ideal low-pass filter, assuming a sampling frequency exceeding the Nyquist rate, as depicted in Fig. 1. Second, since printed images tend to be very large (1440×1440 pixels per square inch), halftoning algorithms need to be of extremely low computational complexity, perhaps implemented in massively parallel processing architectures like GPUs [18]. This second property is particularly important in the context of large graphs where the idea is to sample based on the local graph structure and not the global.

A. Spatial and Spectral Statistics

In order to establish a blue-noise model for sampling signals on a graph, we first propose the idea of a binary dither pattern on a graph, $G = (\mathcal{V}, \mathcal{E})$, as the binary graph signal, $\mathbf{s} \in \{0, 1\}^N$. We refer to the fraction of samples that we intend to

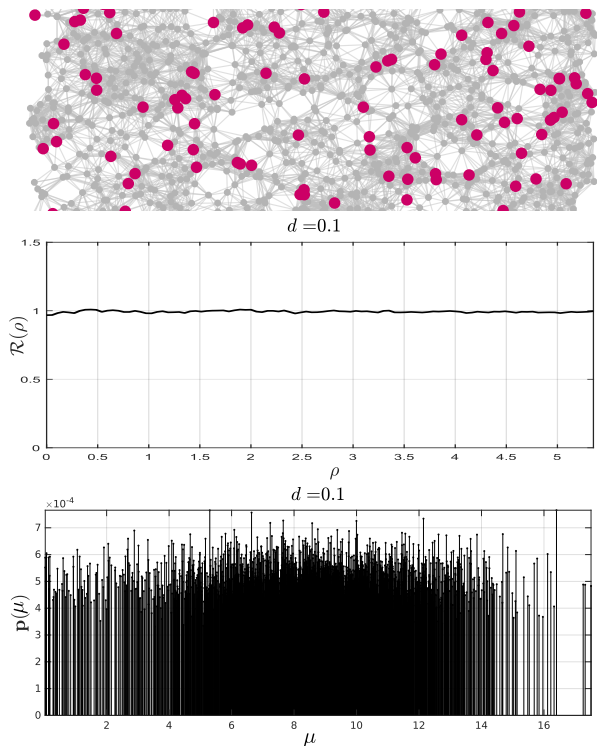


Fig. 2: Illustration of the spatial and spectral properties of (top) a white-noise dither pattern on a Sensor Network graph with density, $d = 0.1$, with (center) a flat pair correlation approximately equal to 1.0 for all internode distances, ρ , and (bottom) an approximately flat power spectra for all frequencies, μ .

preserve as the average density d . In the case of a white-noise dither pattern as illustrated in Fig. 2 (top) on a Sensor Network graph [35] for $d = 0.1$, the components of \mathbf{s} are determined by thresholding a sequence of independent random numbers taken from a uniform distribution in the range of $[0, 1]$ with the pattern density, d , such that each component of \mathbf{s} is a Bernoulli random variable with expected value $\mathbb{E}\{s(\ell)\} = d$ for nodes $\ell \in \{1, \dots, N\}$ and variance $\sigma_s^2 = d(1 - d)$.

Now for the characterization of binary dither patterns, a common spatial metric used in halftoning and borrowed from the study of spatial point processes is the *pair correlation* [18]. This metric attempts to measure the likelihood of neighboring points landing within a series of concentric rings about a given point, but while the idea of concentric rings about a point on a 2D plane is readily understood, the notion is not understood for graphs. As such, we need to define a measure of spacing between neighboring nodes on a graph by defining a path between the nodes v_a and v_b by the *sequence* $(v_a, u_1, u_2, \dots, u_n, v_b)$ where each node in the sequence indicates the nodes visited when going from v_a to v_b , visiting between nodes with edge weights that are different from zero.

Having a sequence of nodes defining a path, we define the length of this path according to:

$$|(v_a, u_1, u_2, \dots, u_n, v_b)| = \mathbf{W}(v_a, u_1) + \mathbf{W}(u_1, u_2) + \dots + \mathbf{W}(u_n, v_b) \quad (10)$$

where the shortest path between two nodes, v_a and v_b , is the

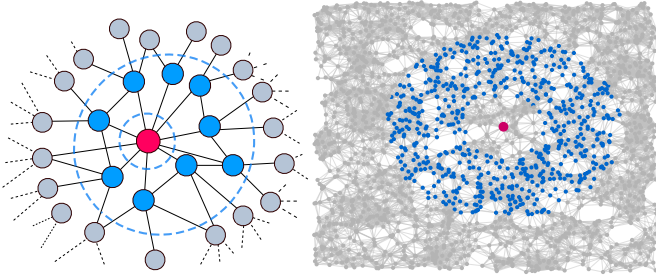


Fig. 3: Illustration of $B_{\Delta}(v, \rho)$ in a graph. The nodes in blue color are located in the annulus of radius ρ and width Δ centered at the node v indicated in red color.

path with minimum length and is represented by γ_{v_a, v_b} . For any $v \in \mathcal{V}$, the *annulus* of radius ρ , width Δ , and center v is defined as $B_{\Delta}(v, \rho) = \{u \in \mathcal{V} : \rho - \Delta \leq |\gamma_{v, u}| < \rho + \Delta\}$. Figure 3 illustrates an example of $B_{\Delta}(v, \rho)$. The symbol $\Gamma \in \mathbb{R}^{N \times N}$ represents the matrix of geodesic distances in the graph, where $\Gamma(u, v) = |\gamma_{u, v}|$.

With a notion of concentric rings in $B_{\Delta}(v, \rho)$, we can now define the pair correlation on a graph. Specifically, if Φ represents a given point process on \mathcal{V} , consider ϕ_s as a realization of Φ associated to the sampling pattern s , such that $\phi_s = \{v \in \mathcal{V} : s(v) = 1\}$ and $\phi_s(\mathcal{S})$ is defined as the number of 1s of s in $\mathcal{S} \subset \mathcal{V}$. The spatial properties of different realizations of Φ can be characterized by the pair correlation function $\mathcal{R}(\rho)$ defined as:

$$\mathcal{R}(\rho) = \frac{\mathbb{E}\{\phi_s(B_{\Delta}(v, \rho)) | s(v) = 1\}}{\mathbb{E}\{\phi_s(B_{\Delta}(v, \rho))\}}, \quad (11)$$

as the influence of a sampling point at node v on all other nodes in the geodesic annular region $B_{\Delta}(v, \rho) = \{u \in \mathcal{V} : \rho - \Delta \leq |\gamma_{v, u}| < \rho + \Delta\}$, where $\mathbb{E}\{\cdot\}$ represents the expectation operator.

Note that for a stationary point process, the unconditional expected number of nodes equal to 1 in the geodesic ring of radius ρ , $\mathbb{E}\{\phi_s(B_{\Delta}(v, \rho))\}$, is approximately given by $d|B_{\Delta}(v, \rho)|$. As such, maxima of $\mathcal{R}(\rho)$ can be considered an indication of the frequent occurrence of the inter-node distance, ρ , between nodes set to 1 whereas minima indicate a reduced occurrence. Returning to our Bernoulli point process, since the expected number of 1s in any annular ring is proportional to the number of nodes within the ring, we expect a pair correlation equal to 1 for all $\rho > 0$ as illustrated in Fig. 2 (center).

Now as an alternative to spatial analysis, it is also possible to characterize the spectral properties of binary dither patterns on a graph where we extend the idea of periodograms to graphs such that the GFTs of q realizations of \mathbf{x} , i.e. $\mathbf{x}_1, \mathbf{x}_2, \dots, \mathbf{x}_q$, are averaged together to form the power spectrum:

$$\mathbf{p}(\ell) = \frac{1}{q} \sum_{i=1}^q \hat{\mathbf{x}}_i(\ell)^2 \quad \ell = 2, \dots, N. \quad (12)$$

Notice that the ℓ^{th} component of \mathbf{p} is associated with the ℓ^{th} eigenvalue μ_{ℓ} . Like its binary halftone counterpart, the GFT of a white-noise sampling pattern is expected to be flat for all μ_k s, and to visualize this power spectra, Fig. 2 (bottom) shows

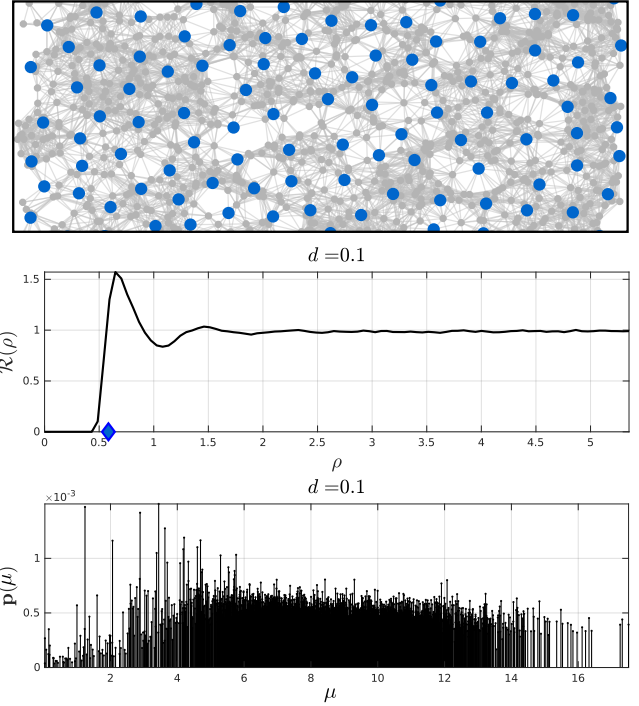


Fig. 4: Illustration of the spatial and spectral properties of (top) a blue-noise dither pattern on a Sensor Network graph with density, $d = 0.1$, with (center) a pair correlation peak at the principal wavelength, λ_b , and (bottom) an approximately high frequency only power spectrum for frequencies, μ .

an estimate of the power spectra for 100 unique white-noise dither patterns generated on the 2000-node Sensor Network graph with pattern density $d = 0.1$.

B. Blue-Noise Graph Signals

Blue-noise halftoning is characterized by a distribution of binary pixels where the minority pixels are spread as homogeneously as possible. Distributing pixels in this manner creates a pattern that is aperiodic, isotropic (radially symmetric), and does not contain any low-frequency spectral components. Halftoning a continuous-tone, discrete-space, monochrome image with blue-noise produces a pattern that, as Ulichney [16] describes, is visually “pleasant” and “does not clash with the structure of an image by adding one of its own, or degrade it by being too ‘noisy’ or uncorrelated.” Similarly on a graph, the minority nodes composing the binary signal are equally spaced apart when measuring distance as the sum of the weights forming the shortest path.

Blue-noise, when applied to an image of constant gray-level g , spreads the minority pixels of the resulting binary image as homogeneously as possible such that the pixels are separated by an average distance, λ_b , referred to as the *principal wavelength* of blue-noise. The value of λ_b is defined as the radius of a round disc, surrounding a minority pixel, such that the ratio of the surface area of a minority pixel to the surface area of the disc is equal to the density of minority pixels, $d = g$ for $0 < g \leq 1/2$ and $d = 1 - g$ for $1/2 < g \leq 1$,

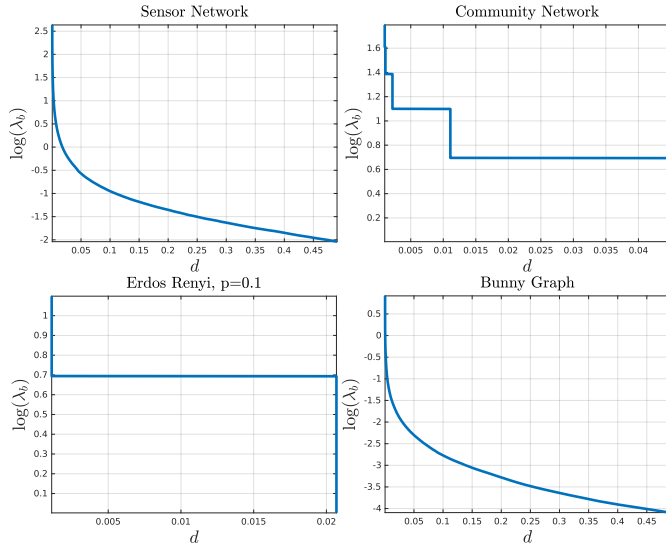


Fig. 5: Calculation of the principal wavelength λ_b versus the density of the sampling pattern for four different graphs traditionally considered in the literature.

which we can write as:

$$d = \frac{D_x D_y}{\lambda_b^2}, \quad (13)$$

where D_x and D_y are the sampling periods (distance between samples) of the digital image in the x and y directions, respectively.

In order to extend the notion of principal wavelength to graphs, we need a notion of surface area as the expected number of graph nodes, $\mathbb{E}\{\mathcal{N}(\lambda)\}$, within a distance or path length, λ , of a given node, and assuming the given node is a minority node. We expect the ratio of our single, minority node to all nodes within a path length, λ_b , to equal the density level according to:

$$d = \frac{1}{\mathbb{E}\{\mathcal{N}(\lambda_b)\}}. \quad (14)$$

Being that $\mathbb{E}\{\mathcal{N}(\lambda_b)\}$ is graph dependent, the graph blue-noise wavelength, λ_b , is likewise graph dependent and its characterization is still an open area of research [36], [37], [38]. In general, one can derive λ_b versus d experimentally as we have in Fig. 5 where we show the principal wavelength versus the density sampling d for some commonly used graphs. We note that in the case of the sensor graph, λ varies smoothly with $d = 1/\mathbb{E}\{\mathcal{N}(\lambda_b)\}$ while, in the case of the community graph, it varies with a piecewise constant behavior with respect to d .

In light of the nature of graph blue-noise to isolate minority nodes, we can begin to characterize blue-noise graph signals in terms of the pair correlation, $\mathcal{R}(\rho)$, by noting that: (a) few or no neighboring minority nodes lie within a path length of $\rho < \lambda_b$; (b) for $\rho > \lambda_b$, the expected number of minority nodes per unit area tends to stabilize around a constant value; and (c) the average number of minority nodes within the path length, ρ , increases sharply nearly λ_b . The resulting pair correlation for blue-noise is, therefore, of the form in

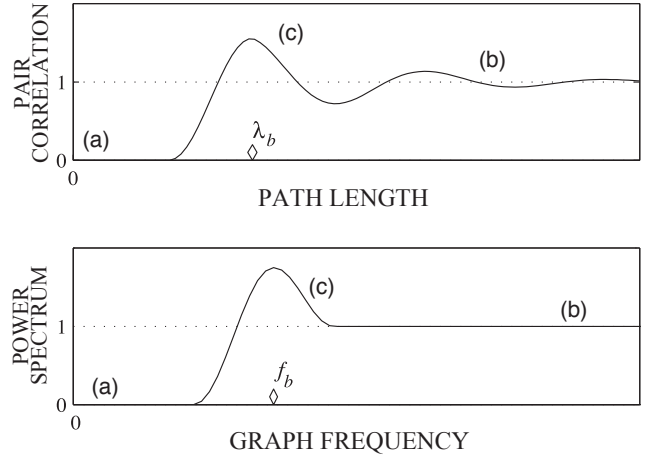


Fig. 6: The ideal (top) pair correlation and (bottom) power spectra for blue-noise graph signals.

Fig. 6 (top), where $\mathcal{R}(\rho)$ shows: (a) a strong inhibition of minority nodes near $\rho = 0$, (b) a decreasing correlation of minority nodes with increasing ρ ($\lim_{\rho \rightarrow \infty} \mathcal{R}(\rho) = 1$), and (c) a frequent occurrence of the inter-node distance λ_b , the principal wavelength, indicated by a series of peaks at integer multiples of λ_b . The principal wavelength is indicated in Fig. 6 (top) by a diamond located along the horizontal axis. Returning to the sample blue-noise signal of Fig. 4 (top), the resulting pair correlation of Fig. 4 (center) has a principal wavelength of $\lambda_b = 0.56$ with a clearly visible peak of 1.55, meaning that nodes equal to 1 are 55% more likely to occur at a distance of $\rho = 0.56$ from an existing 1 than for the unconstrained probability of a node being equal to 1.

Turning to the spectral domain, the spectral characteristics of blue-noise in terms of averaged power spectrum, $\mathbf{p}(\lambda)$, are shown in Fig. 6 (bottom) and can be described by three unique features: (a) little or no low-frequency spectral components; (b) a flat, high-frequency (blue-noise) spectral region; and (c) a peak or concentration of energy at the principal frequency, f_b , equal to the inverse of the principal wavelength; however, a closed form expression between the principal wavelength and the principal frequency on graphs is not available as there is not a closed form expression between the distance between sampling points and the spectral behavior of a sampling pattern. Therefore a specific value of f_b for sampling on graphs is not specified, but from visual inspection, though, there is a peak or concentration of energy separating the low-pass region with little or no energy and the flat high frequency region is illustrated in Fig. 4 (bottom).

C. Blue-noise Sampling Sets

As it has been shown, the binary signal that represents the blue-noise sampling points exhibits a high frequency behavior. Therefore in order to find approximate blue-noise sampling patterns, a cost function is proposed. In particular, we propose a scalar measure of low-frequency energy, R_s , in the signal,

s , as the weighted sum of all Fourier coefficients' energies:

$$R_s = \sum_{\ell=2}^N \frac{\hat{s}^2(\ell)}{\mu_\ell}, \quad (15)$$

which is expected to take a minimum value for blue-noise like sampling patterns. When the minimization of R_s is considered, the vector $[1/\mu_2, 1/\mu_3, \dots, 1/\mu_{N-1}]$ plays the role of a penalty function in which the frequencies are penalized according to the inverse of its value in such a way that the solution of eqn. (15) should be a high-pass signal.

With regards to sampling, Theorem 1 tells us that when a fixed value of the bandwidth ω is considered and a signal has to be sampled taking m samples, it is necessary to look for the set of nodes, \mathcal{S} , such that \mathcal{S}^c is a $\Lambda_{\mathcal{S}^c}$ -removable set with $\omega < \Lambda_{\mathcal{S}^c}$. Finding the subset of m nodes with the maximum $\Lambda_{\mathcal{S}^c}$ would, therefore, give the *best sampling set*. On the other hand, if a signal has to be sampled taking a number of m samples, choosing a set of nodes \mathcal{S} with the maximum value of $\Lambda_{\mathcal{S}^c}$ will extend the class of signals, $PW_\omega(G)$, that can be sampled and represented in a unique way with m samples.

Now if one can show that minimizing the redness in a sampling signal promotes high values of $\Lambda_{\mathcal{S}^c}$, one could argue blue-noise was a desirable attribute for efficient sampling. The following theorem establishes this relationship:

Theorem 3

Let $s : \mathcal{V} \rightarrow \{0, 1\}$ be a sampling pattern with $s|_{\mathcal{S}} = 1$, $s|_{\mathcal{S}^c} = 0$ for $\mathcal{S} \subset \mathcal{V}$ and $|\mathcal{S}| = \|s\|_0 = m$, then the $\Lambda_{\mathcal{S}^c}$ -constant of the set \mathcal{S}^c satisfies

$$\Lambda_{\mathcal{S}^c} > C_\delta \left(\frac{R_s}{\text{vol}(G)R_s - m^2 \left(1 - \frac{m}{N}\right)^2} \right)^{\frac{2}{5}} \quad (16)$$

where R_s is the redness in s from eqn. (15);

$$\text{vol}(G) = \sum_{v=1}^N \mathbf{D}(v, v); \quad (17)$$

δ is the isoperimetric dimension of G [27], [39]; and C_δ a constant that depends only on δ .

Proof: See Appendix A.

To summarize, Theorem 1 tells us that the best sampling set, \mathcal{S} , is the one for which the value of $\Lambda_{\mathcal{S}^c}$ is a maximum; therefore while blue-noise sampling patterns (which minimize R_s) are not necessarily the *best* sampling sets, they are *good* sampling sets in comparison with a totally random selection of the nodes. Notice that eqn. (16) is well defined as $\text{vol}(G)R_s - m^2 \left(1 - \frac{m}{N}\right)^2 > 0$, which is tight when $\mathcal{S}^c \cup b\mathcal{S}^c = \mathcal{V}$ where $b\mathcal{S}^c$ is the boundary of \mathcal{S}^c . This criteria can be satisfied making the nodes in \mathcal{S} as spread apart as possible in the graph, which is reasonable as a sampling set where all the nodes are too concentrated in one area could lead to poor reconstructions of signals that exhibit fast changes in the sparsely sampled areas left elsewhere.

As an approach to reinforce the benefits of blue-noise sampling sets, we can use Theorem 2 to show how blue-noise promotes those sampling sets that maximize the bandwidth of

the signals that can be represented in a unique way on a given sampling set as indicated in the following theorem:

Theorem 4

Let $s : \mathcal{V} \rightarrow \{0, 1\}$ with $s|_{\mathcal{S}} = 1$, $s|_{\mathcal{S}^c} = 0$, $\mathcal{S} \subset \mathcal{V}$. If $K_{\mathcal{S}} > 0$, then

$$K_{\mathcal{S}} \geq \left(\frac{m^2 \left(1 - \frac{m}{N}\right)^2}{R_s - \gamma} \right)^{1/2} \quad (18)$$

where

$$\gamma = \max_{\mathcal{S}, v', v} \left(\sum_{v \in \mathcal{S}^c \setminus v'} w_{\mathcal{S}}(v)^2 \right).$$

and R_s is, again, the redness in s from eqn. (15).

Proof: See Appendix B

What Theorem 4 says is that lowering the redness of the sampling pattern raises the minimum possible value of $K_{\mathcal{S}}$ and, therefore, extends the set of signals, $PW_\omega(G)$, that can be represented in a unique way on a given sampling set. So again, the blue-noise sampling patterns that are characterized by small values of R_s represent a better option than arbitrary random sampling, which leads to large values of R_s .

IV. GENERATING BLUE-NOISE SAMPLING SETS

Given that blue-noise graph signal sampling promotes the finding of good sampling sets, it is natural to ask how such sampling patterns can be generated. An algorithm that has been particularly successful in digital halftoning and that intuitively translates to graphs is the Void-And-Cluster (VAC) algorithm, introduced by Ulichney [25]. VAC allows for the construction of artifact-free homogeneous dithering patterns by iteratively measuring the concentration of minority pixels in a binary halftone image, using a gaussian low-pass filter, and swapping the minority pixel in the area of highest concentration with the non-minority pixel in the area of lowest concentration. The adaptation of this algorithm to sampling signals on graphs consists roughly speaking of the sequential computation of distances between sampling points in such a way that points with short geodesic distances between them are relocated trying to put them far from each other.

In order to exploit the above principle for the selection of sampling nodes on a graph, a Gaussian kernel $\mathbf{K}(u, v) = \exp(-\Gamma(u, v)^2/\sigma)$ is evaluated on the set of geodesic distances, Γ . This provides a new set of distances that can be tuned according to the parameter, σ , where a small value of $\Gamma(u, v)$ leads to a value of $\mathbf{K}(u, v)$ that is close to unity while a large value of $\Gamma(u, v)$ leads to a value of $\mathbf{K}(u, v)$ close to zero. As a measure of how homogeneously distributed the sampling points are, the sum of all distances from one node to the others via the kernel \mathbf{K} is calculated as $\mathbf{c} = \mathbf{K}\mathbf{1}_{N \times 1}$. With this, an initial sampling pattern is generated selecting the m components of \mathbf{c} with lowest value where $m = dN$ is the number of 1's in the sampling pattern with density d . The purpose of this initial choice is to select those nodes that are far apart as possible from each other.

The components of \mathbf{c} whose index is given by the location of the 1's in s , are then updated to be

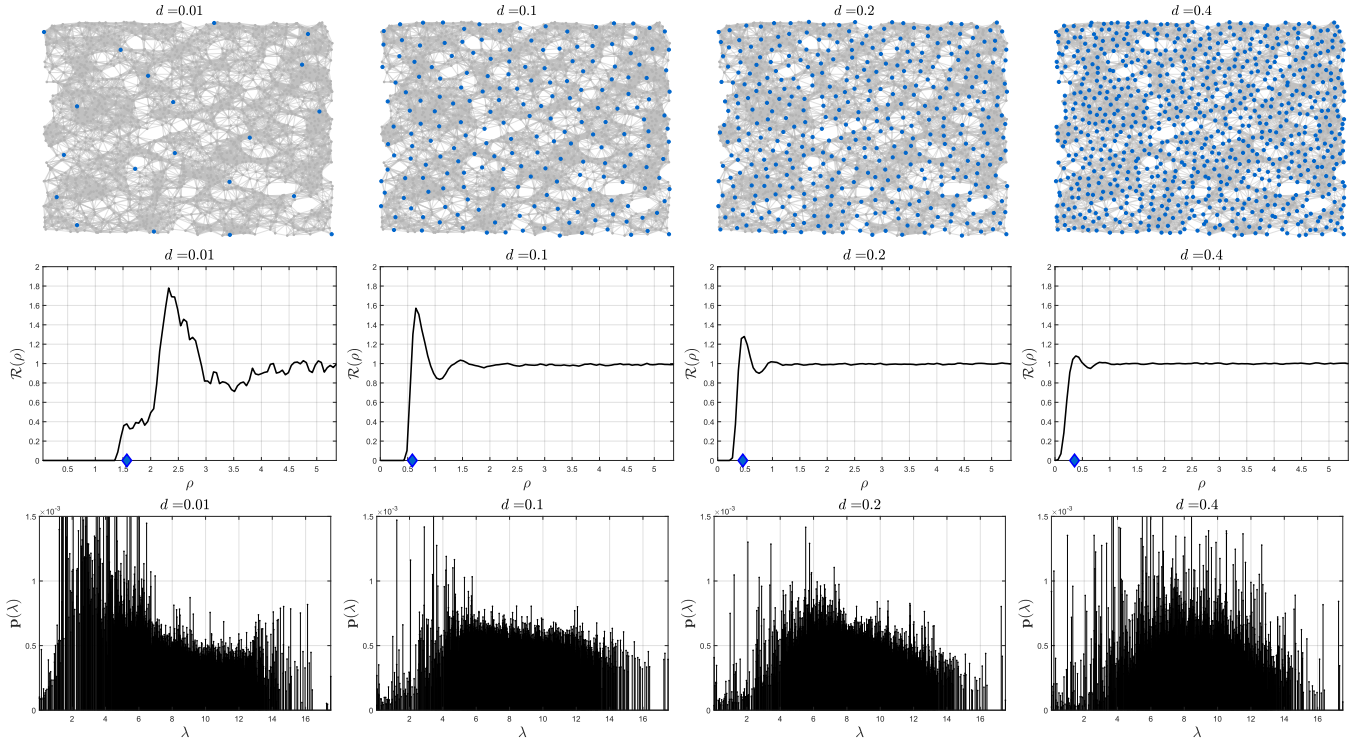


Fig. 7: Void and cluster: blue-noise sampling patterns for different intensities d . First row: Localization on the graph of the nodes selected in a blue-noise sampling pattern. Second row: The pair correlation function $\mathcal{R}(\rho)$ for the sampling patterns indicating with a diamond marker the value of λ_b . Third row: Power spectral density for the different blue-noise sampling patterns.

$\mathbf{c}(\text{supp}(s)) = \sum \mathbf{K}(\text{supp}(s), \text{supp}(s))$, and the remaining components of \mathbf{c} are updated according to $\mathbf{c}(\text{supp}(s)^c) = \sum \mathbf{K}(\text{supp}(s), \text{supp}(s)^c) - \tau$, where τ is selected as a large scalar value. This update allows to represent as positive quantities the distances between the sampling points in the pattern without adding the distances to other nodes. The distance between $\text{supp}(s)$ and $\text{supp}(s)^c$ is then represented with a negative value. Now the index of the component of \mathbf{c} with the highest value will indicate the sampling point that is closest to the other sampling points, and then the value of s at that index is forced to be 0 whereas the index where \mathbf{c} is minimum is forced to be 1.

Repeating the above process iteratively, it is possible to achieve a sampling pattern with no clusters of 1s that exhibits a homogeneous distribution on \mathcal{V} . The details of the VAC algorithm can be appreciated in Algorithm 1 with example sampling patterns using VAC depicted in Fig. 7 for the Sensor Network graph. From observation, one can see a clear distinction with respect to random sampling when it comes to the nodes distribution of the sampling set. The spatial and spectral blue-noise-like behavior is obtained as a byproduct of the algorithm.

At this point, we note that the value of σ in the kernel $\exp(-\Gamma(u, v)^2/\sigma)$ plays a critical role in VAC as it defines which sampling nodes are close enough to another one in order to produce a relocation of the 1's in the sampling pattern. Taking into account the definition of λ_b presented

in previous sections, it is possible to establish a natural connection between σ and λ_b . In order to do so, we note that if the blue noise sampling pattern is ideally distributed on the set of nodes, \mathcal{V} , then when u and v are sampling nodes it follows that $\exp(-\Gamma(u, v)^2/\sigma) \approx 0$ if $\Gamma(u, v) \geq \lambda_b$. This criteria is considered to be satisfied when $\sigma = \lambda_b^2/\ln(10)$, i.e selecting σ in this way the exponential reaches a value of 0.1 when $\Gamma(u, v) = \lambda_b$.

Now unlike in traditional halftoning, a general result for any graph stating the relationship between power spectrum of a sampling pattern and the geodesic distance among sampling points is not available. This can be explained by the variety of graphs in which the weights are arbitrarily defined and can have different physical meanings. As indicated in Fig. 8, there is a clear reduction of the redness of the patterns as they get better distributed on the nodes of the graph. It is important to mention that this tendency is even more clear as the value of d is reduced. This is related with the fact that as d is reduced there are more possibilities for the relocation of the 1's in the sampling pattern.

V. EXPERIMENTS

In order to evaluate the benefits of blue noise sampling a set of numerical experiments is performed comparing the obtained results against state of the art techniques. The simulations are performed considering different graphs and signal models. The experiment is described by the following steps:

Algorithm 1 Void and cluster algorithm for graphs**Input:** m : number of samples, σ .**Output:** s : sampling pattern*Initialisation* : $s = \mathbf{0}$, $\text{IndA}=-1$, $\text{IndB}=-1$.Calculate $\mathbf{K}(i, j) = e^{-\frac{\Gamma(i, j)^2}{\sigma}}$ for all $1 \leq i, j \leq N$.2: $\mathbf{c} = \mathbf{K}\mathbf{1}_{N \times 1}$.Get \mathcal{M} as the indexes of the m lowest components of \mathbf{c} .4: $s(\mathcal{M}) = 1$.**for** $r = 1 : 1 : N$ **do**6: $\mathbf{c}(\text{supp}(s)) = \sum \mathbf{K}(\text{supp}(s), \text{supp}(s))$. $\mathbf{c}(\text{supp}(s)^c) = \sum \mathbf{K}(\text{supp}(s), \text{supp}(s)^c) - \tau$.8: $s(\arg \max_i \{\mathbf{c}(i)\}) = 0$. $s(\arg \min_i \{\mathbf{c}(i)\}) = 1$.10: **if** $\text{IndA}=\arg \max_i \{\mathbf{c}(i)\}$ and $\text{IndB}=\arg \min_i \{\mathbf{c}(i)\}$ **then**

break

12: **else**IndA= $\arg \min_i \{\mathbf{c}(i)\}$.14: IndB= $\arg \max_i \{\mathbf{c}(i)\}$.**end if**16: **end for****return** s

- For each graph model, a set of 100 signals is generated according to the specific signal models selected.
- Each signal is sampled by means of different sampling schemes.
- The signal reconstructed from the samples is compared to the original one and its mean squared error (MSE) is calculated.
- The values of the MSE are averaged over 100.

The schemes of sampling considered for the experiment are the following:

- Blue noise sampling by void and cluster.
- Sampling scheme proposed by Chen et. al. [15].
- Sampling scheme proposed by Anis et. al. [31].

The signal models are:

- Signal model 1 (SM1): A random signal of bandwidth $k = 50$, where the Fourier coefficients are generated from the Gaussian distribution $\mathcal{N}(0, 0.5^2)$. The samples captured are contaminated with additive Gaussian noise such that the Signal to Noise Ratio is $SNR = 20\text{dB}$.
- Signal model 2 (SM2): A random signal of bandwidth $k = 50$, where the nonzero Fourier coefficients are generated from the Gaussian distribution $\mathcal{N}(0, 0.5^2)$. This signal is modulated on the spectral axes by $h(\lambda)$, where

$$h(\lambda) = \begin{cases} 1 & \text{If } \lambda \leq \lambda_{50} \\ e^{-4(\lambda - \lambda_{50})} & \text{If } \lambda > \lambda_{50} \end{cases} \quad (19)$$

The graphs considered in the simulations are different from each other in their nature and represent typical graphs that can be found in different scenarios and applications. The graph models used are:

- Graph G_1 : A random sensor network with $N = 1000$ nodes. The weights in the graph are given by the Euclidean distance

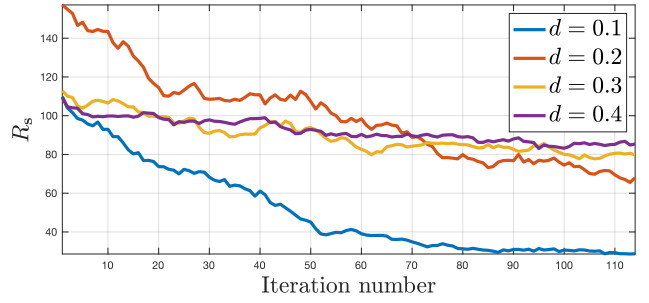


Fig. 8: Illustration of the redness, $R_s = \sum_{\ell=2}^N \frac{\hat{s}(\ell)^2}{\mu_\ell}$, of the void and cluster blue noise sampling patterns on a sensor network with $N = 2000$ nodes, considering different densities.

between points. The maximum number of neighbors for each node is 6.

- Graph G_2 : A community graph with $N = 1000$ nodes, 16 communities generated using the GSP toolbox [35].
- Graph G_3 : A Barabási-Albert random network [4] with $N = 1000$ nodes.

In Fig. 9, the performance of different algorithms can be appreciated including VAC sampling. Notice that the decay rate of the error curves show consistently the benefits of blue noise sampling. In the particular case of graph G_1 , VAC sampling offers the lowest error for both signal models. In the case of graphs G_2 and G_3 , the results obtained using VAC are close to the ones obtained in [31].

VI. CONCLUSION

In this paper, we propose a definition of blue-noise sampling on graphs based on the traditional blue-noise model associated with digital halftones. The properties and benefits of blue-noise sampling on graphs are linked with theoretical results related to uniqueness sets in sampling, showing why blue-noise patterns promote good sampling sets. We also extended a popular halftoning scheme to generating blue-noise sample sets on graphs. Numerical tests on different graphs corroborate the good qualities of sampling with blue-noise. We further note that the results obtained in this work can be extended for specific families of graphs. The delimitation of the properties for the graphs under consideration could lead to sharper bounds and could allow the definition of other quantities extensively used in halftoning, like the principal frequency.

Perhaps an overlooked benefit to blue-noise sampling is the wealth of computationally efficient algorithms used in digital halftones that can be extended to graph sampling without spectral estimation, namely error-diffusion where the produced halftone patterns conform to the local spectral content of the image to optimally preserve salient features like edges, gradients, flood fills, etc. Also a very valuable attribute of error-diffusion that is not widely recognized outside the halftoning community is that error-diffusion can be trained to produce arbitrary spectral profiles (blue-noise, green-noise, etc) and even designed to match the dither patterns produced by other means, including ones with high computational complexity [17], [20]. For graph signal sampling, this opens up

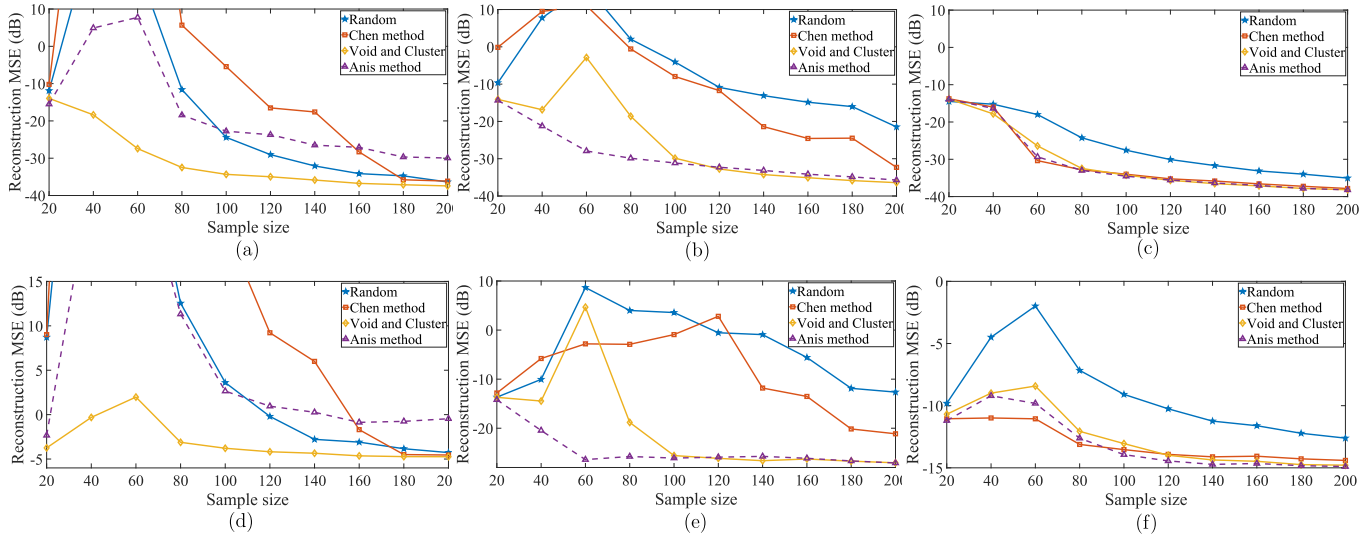


Fig. 9: Averaged MSE vs the sampling rate considering the reconstruction of 100 different signals from its samples using several sampling schemes and considering several graphs: (a) The graph G_1 and the signal model SM1. (b) The graph G_2 and the signal model SM1. (c) The graph G_3 and the signal model SM1. (d) The graph G_1 and the signal model SM2. (e) The graph G_2 and the signal model SM2. (f) The graph G_3 and the signal model SM2.

the possibility of error-diffusion algorithms trained to mimic sampling algorithms based on spectral estimation. \square

APPENDIX A PROOF OF THEOREM 3

In order to prove Theorem 3, some preliminary lemmas and theorems are discussed.

Theorem 5 (Jensens)

For a real convex function F , numbers x_1, x_2, \dots, x_n in the domain of F and positive weights a_i it follows that

$$F\left(\frac{\sum_i a_i x_i}{\sum_i a_i}\right) \leq \frac{\sum_i a_i F(x_i)}{\sum_i a_i}. \quad (20)$$

Lemma 6

Let $s \in \{0, 1\}^N$ a binary signal on \mathcal{V} with $\|s\|_0 = m$. Then, it holds that:

$$\frac{1}{\sum_{\ell=2}^N \hat{s}(\ell)^2 \mu_\ell} \leq \frac{1}{m^2 \left(1 - \frac{m}{N}\right)^2} \sum_{\ell=2}^N \frac{\hat{s}(\ell)^2}{\mu_\ell} \quad (21)$$

Proof. Considering Jensens inequality in theorem 5 with $F = 1/u$ for $u > 0$ it is possible to get

$$\frac{\sum_{\ell=2}^N \hat{s}(\ell)^2}{\sum_{\ell=2}^N \hat{s}(\ell)^2 \mu_\ell} \leq \frac{\sum_{\ell=2}^N \hat{s}(\ell)^2 \frac{1}{\mu_\ell}}{\sum_{\ell=2}^N \hat{s}(\ell)^2} \quad (22)$$

and taking into account that $\sum_{\ell=1}^N \hat{s}(\ell)^2 = \hat{s}^T \hat{s} = s^T s = m$, and $\hat{s}(1) = (1/\sqrt{N})\mathbf{1}^T s = m/\sqrt{N}$, it follows that

$$\frac{1}{\sum_{\ell=2}^N \hat{s}(\ell)^2 \mu_\ell} \leq \frac{1}{m^2 \left(1 - \frac{m}{N}\right)^2} \sum_{\ell=2}^N \frac{\hat{s}(\ell)^2}{\mu_\ell}. \quad (23)$$

Lemma 7

For any subset of nodes $\mathcal{S} \subset \mathcal{V}$ and sampling pattern $s \in \{0, 1\}^N$ with $\text{supp}(s) = \mathcal{S}$, it follows that

$$\text{vol}(\mathcal{S}) \geq \frac{m^2 \left(1 - \frac{m}{N}\right)^2}{\sum_{\ell=2}^N \frac{1}{\mu_\ell} \hat{s}(\ell)^2} \quad (24)$$

where $m = \|s\|_0 = |\mathcal{S}|$.

Proof. Lets consider the Laplacian matrix \mathbf{L} . Multiplying on the left by s^T and on the right hand side by s it follows that $s^T \mathbf{L} s = s^T \mathbf{D} s - s^T \mathbf{W} s$, which leads to

$$\sum_{\ell=2}^N \mu_\ell \hat{s}(\ell)^2 = \text{vol}(\mathcal{S}) - s^T \mathbf{W} s$$

and therefore

$$\sum_{\ell=2}^N \mu_\ell \hat{s}(\ell)^2 \leq \text{vol}(\mathcal{S}).$$

Now, taking into account the Lemma 6 it follows that

$$\text{vol}(\mathcal{S}) \geq \frac{m^2 \left(1 - \frac{m}{N}\right)^2}{\sum_{\ell=2}^N \frac{1}{\mu_\ell} \hat{s}(\ell)^2} \quad \square$$

A. Proof of Theorem 3

Proof. Fuhr and Pesenson [27] show that if a subset of nodes $\mathcal{U} \subset \mathcal{V}$ is removable with constant $\Lambda_{\mathcal{U}}$, it follows that $\Lambda_{\mathcal{U}} \geq \mu_D(\mathcal{U})$, where $\mu_D(\mathcal{U})$ is the Dirichlet eigenvalue of

the induced subgraph¹ of \mathcal{U} . This inequality is tight always that $\mathcal{U} \cup b\mathcal{U} = \mathcal{V}$, where $b\mathcal{U}$ is the vertex boundary of \mathcal{U} .

As stated in [27], $\mu_D(\mathcal{U})$ satisfy the following inequality

$$\mu_D(\mathcal{U}) > C_\delta \left(\frac{1}{\text{vol}(\mathcal{U})} \right)^{2/\delta} \quad (25)$$

where δ is the isoperimetric dimension of the graph, C_δ is a constant that depends only on δ and $\text{vol}(\mathcal{U}) = \sum_{v \in \mathcal{U}} D(v, v)$.

Now, taking into account that $\text{vol}(G) = \text{vol}(\mathcal{S}) + \text{vol}(\mathcal{S}^c)$ for any $\mathcal{S} \subset \mathcal{V}$, and the lemma 7, we have that

$$\text{vol}(G) - \text{vol}(\mathcal{S}) \leq \text{vol}(G) - \frac{m^2 \left(1 - \frac{m}{N}\right)^2}{\sum_{\ell=2}^N \frac{1}{\mu_\ell} \hat{\mathbf{s}}(\ell)^2} \quad (26)$$

and then

$$C_\delta \left(\frac{1}{\text{vol}(G) - \text{vol}(\mathcal{S})} \right)^{\frac{2}{\delta}} \geq C_\delta \left(\frac{\sum_{\ell=2}^N \frac{1}{\mu_\ell} \hat{\mathbf{s}}(\ell)^2}{\text{vol}(G) \sum_{\ell=2}^N \frac{1}{\mu_\ell} \hat{\mathbf{s}}(\ell)^2 - m^2 \left(1 - \frac{m}{N}\right)^2} \right)^{\frac{2}{\delta}}. \quad (27)$$

Now, taking into account that $\Lambda_{\mathcal{S}^c} \geq \mu_D(\mathcal{S}^c)$, it follows that

$$\Lambda_{\mathcal{S}^c} \geq C_\delta \left(\frac{\sum_{\ell=2}^N \frac{1}{\mu_\ell} \hat{\mathbf{s}}(\ell)^2}{\text{vol}(G) \sum_{\ell=2}^N \frac{1}{\mu_\ell} \hat{\mathbf{s}}(\ell)^2 - m^2 \left(1 - \frac{m}{N}\right)^2} \right)^{\frac{2}{\delta}} \quad (28)$$

□

APPENDIX B PROOF OF THEOREM 4

In this section the proof of Theorem 4 is provided. Before this proof is presented an important lemma is introduced.

Lemma 8

Let $\mathbf{s} : \mathcal{V} \mapsto \{0, 1\}^N$ a binary signal defined on \mathcal{V} and let $\bar{\mathbf{s}} = \mathbf{1} - \mathbf{s}$, then it follows that

$$\sum_{\ell=2}^N \mu_\ell \hat{\hat{\mathbf{s}}}(\ell)^2 = \sum_{\ell=2}^N \mu_\ell \hat{\mathbf{s}}(\ell)^2 \quad (29)$$

Proof. Lets consider the Laplacian matrix \mathbf{L} and multiply on the left by \mathbf{s}^\top and on the right by \mathbf{s} , it follows that

$$\mathbf{s}^\top \mathbf{L} \mathbf{s} = (\mathbf{1} - \bar{\mathbf{s}})^\top \mathbf{L} (\mathbf{1} - \bar{\mathbf{s}}) = \bar{\mathbf{s}}^\top \mathbf{L} \bar{\mathbf{s}}. \quad (30)$$

Now, taking into account that $\mathbf{x}^\top \mathbf{L} \mathbf{x} = \sum_{\ell=1}^N \mu_\ell \hat{\mathbf{x}}(\ell)^2$, it follows that

$$\sum_{\ell=2}^N \mu_\ell \hat{\hat{\mathbf{s}}}(\ell)^2 = \sum_{\ell=2}^N \mu_\ell \hat{\mathbf{s}}(\ell)^2. \quad (31)$$

Notice that $\mu_1 = 0$ and consequently the sum can be computed for $\ell \geq 2$. □

¹Definitions and inequalities about induced subgraphs can be found in [39]

A. Proof of Theorem 4

Proof. Taking into account that

$$(\mathbf{L} \mathbf{x})(v) = \sum_{u \in \mathcal{V}} (\mathbf{x}(v) - \mathbf{x}(u)) \mathbf{W}(v, u) \quad (32)$$

and $w_{\mathcal{S}}(v) = \sum_{u \in \mathcal{S}} \mathbf{W}(u, v)$. It is possible to infer that

$$(\mathbf{L} \bar{\mathbf{s}})(v) = \begin{cases} w_{\mathcal{S}}(v) & \text{if } v \in \mathcal{S}^c \\ -w_{\mathcal{S}^c}(v) & \text{if } v \in \mathcal{S} \end{cases} \quad (33)$$

where $\bar{\mathbf{s}} = \mathbf{1} - \mathbf{s}$. Now, taking into account equation (33) and Lemma 8 it follows that

$$\bar{\mathbf{s}}^\top \mathbf{L} \bar{\mathbf{s}} = \sum_{\ell=2}^N \mu_\ell \hat{\hat{\mathbf{s}}}(\ell)^2 = \sum_{v \in \mathcal{S}^c} w_{\mathcal{S}}^2(v)$$

$$\sum_{\ell=2}^N \mu_\ell \hat{\mathbf{s}}(\ell)^2 = K_{\mathcal{S}}^2 + \sum_{v \in \{\mathcal{S}^c \setminus v'\}} w_{\mathcal{S}}(v)^2$$

$$K_{\mathcal{S}} = \left(\sum_{\ell=2}^N \mu_\ell \hat{\mathbf{s}}(\ell)^2 - \sum_{v \in \{\mathcal{S}^c \setminus v'\}} w_{\mathcal{S}}(v)^2 \right)^{\frac{1}{2}}$$

which leads to

$$K_{\mathcal{S}} \geq \left(\sum_{\ell=2}^N \mu_\ell \hat{\mathbf{s}}(\ell)^2 - \gamma \right)^{\frac{1}{2}}$$

where γ is given by

$$\gamma = \max_{\mathcal{S}, v, v'} \sum_{v \in \{\mathcal{S}^c \setminus v'\}} w_{\mathcal{S}}(v)^2 \quad (34)$$

and taking into account Lemma 6, it follows that

$$K_{\mathcal{S}} \geq \left(\frac{m^2 \left(1 - \frac{m}{N}\right)^2}{\sum_{\ell=2}^N \frac{1}{\mu_\ell} \hat{\mathbf{s}}(\ell)^2} - \gamma \right)^{\frac{1}{2}}$$

□

REFERENCES

- [1] F.S. Roberts. *Graph Theory and Its Applications to Problems of Society*. CBMS-NSF Regional Conference Series in Applied Mathematics. Society for Industrial and Applied Mathematics, 1978.
- [2] André A. Keller. Graph theory and economic models: from small to large size applications. *Electronic Notes in Discrete Mathematics*, 28(Supplement C):469 – 476, 2007. 6th Czech-Slovak International Symposium on Combinatorics, Graph Theory, Algorithms and Applications.
- [3] A. Fornito, A. Zalesky, and E. Bullmore. *Fundamentals of Brain Network Analysis*. Elsevier Science, 2016.
- [4] A.L. Barabási and M. Pósfai. *Network Science*. Cambridge University Press, 2016.
- [5] D. I. Shuman, S. K. Narang, P. Frossard, A. Ortega, and P. Vandergheynst. The emerging field of signal processing on graphs: Extending high-dimensional data analysis to networks and other irregular domains. *IEEE Signal Processing Magazine*, 30(3):83–98, May 2013.
- [6] David I Shuman, Benjamin Ricaud, and Pierre Vandergheynst. Vertex-frequency analysis on graphs. *Applied and Computational Harmonic Analysis*, 40(2):260 – 291, 2016.
- [7] David I Shuman, Mohammad Javad Faraji, and Pierre Vandergheynst. A multiscale pyramid transform for graph signals. *IEEE Transactions on Signal Processing*, 64(8):2119–2134, 2016.
- [8] B.I. Goldengorin, V.A. Kalyagin, and P.M. Pardalos. *Models, Algorithms, and Technologies for Network Analysis: Proceedings of the First International Conference on Network Analysis*. Springer Proceedings in Mathematics & Statistics. Springer New York, 2012.

- [9] S. S. Ray. *Graph Theory with Algorithms and its Applications: In Applied Science and Technology*. Springer India, 2012.
- [10] D. Jungnickel. *Graphs, Networks and Algorithms*. Algorithms and Computation in Mathematics. Springer Berlin Heidelberg, 2012.
- [11] I. Z. Pesenson. Sampling solutions of schrodinger equations on combinatorial graphs. In *2015 International Conference on Sampling Theory and Applications (SampTA)*, pages 82–85, May 2015.
- [12] Isaac Z. Pesenson and Meyer Z. Pesenson. Sampling filtering and sparse approximations on combinatorial graphs. *Journal of Fourier Analysis and Applications*, 16(6):921–942, Dec 2010.
- [13] A. Ortega, P. Frossard, J. Kovačević, J. M. F. Moura, and P. Vandergheynst. Graph Signal Processing. *ArXiv e-prints*, December 2017.
- [14] A. Anis, A. Gadde, and A. Ortega. Towards a sampling theorem for signals on arbitrary graphs. In *2014 IEEE International Conference on Acoustics, Speech and Signal Processing (ICASSP)*, pages 3864–3868, May 2014.
- [15] S. Chen, R. Varma, A. Sandryhaila, and J. Kovaevi. Discrete signal processing on graphs: Sampling theory. *IEEE Transactions on Signal Processing*, 63(24):6510–6523, Dec 2015.
- [16] R. A. Ulichney. Dithering with blue noise. *Proceedings of the IEEE*, 76(1):56–79, 1988.
- [17] D. L. Lau, R. Ulichney, and G. R. Arce. Blue and green noise half-toning models. *IEEE Signal Processing Magazine*, 20(4):28–38, July 2003.
- [18] D. Lau and G. R. Arce. *Modern digital half-toning*. CRC Press, 2 edition, 2008.
- [19] D. L. Lau, A. M. Khan, and G. R. Arce. Stochastic moiré. In *IS&T's PICS 2001: Image Processing, Image Quality, Image Capture Systems Conference*, pages 96–100, Montréal, Quebec, Canada, April 22-25 2001.
- [20] D. L. Lau, G. R. Arce, and N. C. Gallagher. Digital color half-toning with generalized error diffusion and multichannel green-noise masks. *IEEE Transactions on Image Processing*, 9(5):923–935, May 2000.
- [21] J. Bacca Rodriguez, G. R. Arce, and D. L. Lau. Blue-noise multitone dithering. *IEEE Transactions on Image Processing*, 17(8):1368–1382, Aug 2008.
- [22] Daniel L. Lau, Gonzalo R. Arce, and Neal C. Gallagher. Digital half-toning by means of green-noise masks. *J. Opt. Soc. Am. A*, 16(7):1575–1586, Jul 1999.
- [23] S.N. Chiu, D. Stoyan, W.S. Kendall, and J. Mecke. *Stochastic Geometry and Its Applications*. Wiley series in probability and statistics. 2013.
- [24] F. Marvasti. *Nonuniform Sampling: Theory and Practice*. Number v. 1 in Information Technology Series. Springer US, 2001.
- [25] Robert A. Ulichney. Void-and-cluster method for dither array generation, 1993.
- [26] A. Sandryhaila and J. M. F. Moura. Discrete signal processing on graphs. *IEEE Transactions on Signal Processing*, 61(7):1644–1656, April 2013.
- [27] Hartmut Fuhr and Isaac Z. Pesenson. Poincaré and Plancherel polyadic inequalities in harmonic analysis on weighted combinatorial graphs. *SIAM Journal on Discrete Mathematics*, 27(4):2007–2028, 2013.
- [28] Gilles Puy, Nicolas Tremblay, Rmi Gribonval, and Pierre Vandergheynst. Random sampling of bandlimited signals on graphs. *Applied and Computational Harmonic Analysis*, 44(2):446 – 475, 2018.
- [29] D. I. Shuman, M. J. Faraji, and P. Vandergheynst. A multiscale pyramid transform for graph signals. *IEEE Transactions on Signal Processing*, 64(8):2119–2134, April 2016.
- [30] T. Biyikoglu, J. Leydold, and P.F. Stadler. *Laplacian Eigenvectors of Graphs: Perron-Frobenius and Faber-Krahn Type Theorems*. Lecture Notes in Mathematics. Springer Berlin Heidelberg, 2007.
- [31] A. Anis, A. Gadde, and A. Ortega. Efficient sampling set selection for bandlimited graph signals using graph spectral proxies. *IEEE Transactions on Signal Processing*, 64(14):3775–3789, July 2016.
- [32] Nicolas Tremblay, Pierre-Olivier Amblard, and Simon Barthélemy. Graph sampling with determinantal processes. *CoRR*, abs/1703.01594, 2017.
- [33] Luca Avena and Alexandre Gaudillire. On some random forests with determinantal roots. 10 2013.
- [34] A. G. Marques, S. Segarra, G. Leus, and A. Ribeiro. Sampling of graph signals with successive local aggregations. *IEEE Transactions on Signal Processing*, 64(7):1832–1843, April 2016.
- [35] Nathanael Perraudin, Johan Paratte, David I. Shuman, Vassilis Kalofolias, Pierre Vandergheynst, and David K. Hammond. GSPBOX: A toolbox for signal processing on graphs. *CoRR*, abs/1408.5781, 2014.
- [36] V. de Silva and R. Ghrist. Coordinate-free coverage in sensor networks with controlled boundaries via homology. *The International Journal of Robotics Research*, 25(12):1205–1222, 2006.
- [37] Vin de Silva and Robert Ghrist. Coverage in sensor networks via persistent homology. *Algebr. Geom. Topol.*, 7(1):339–358, 2007.
- [38] V. De Silva and R. Ghrist. Homological sensor networks. *Notices Amer. Math. Soc.*, pages 10–17, 2007.
- [39] F.R.K. Chung. *Spectral Graph Theory*. Number no. 92 in CBMS Regional Conference Series. American Mathematical Society, 1997.